First-look enabled Autonomous Aerial Visual Inspection of Geometrically Fractured Objects in Constrained Environments

Vignesh Kottayam Viswanathan, Sumeet Gajanan Satpute, Björn Lindqvist, and George Nikolakopoulos

2022 IEEE 31st International Symposium on Industrial Electronics (ISIE) | 978-1-6654-8240-0/22/$31.00 ©2022 IEEE | DOI: 10.1109/ISIE51582.2022.9831615

***Abstract*—In this article we propose a novel offline, model-based aerial visual inspection scheme for geometrically fractured large objects, based on fully autonomous Unmanned Aerial Vehicles (UAVs), while specifically targeting the case of constrained environments. The proposed framework enables a safe and collision free inspection mission, while guaranteeing a complete visual inspection of the object of interest. The proposed framework employs a novel $First - Look$ approach to generate viewpoints satisfying specific photogrammetric requirements, as well as spatial constraints that are inherently applied by the UAV's state constraints. As it will be presented, i) the $First - Look$ approach allows the UAV to first orient it's view vector towards the nearest available point detected by $kd - tree$ based Nearest Neighbour search on the object, from it's current position, and ii) in the sequel, based on the orientation of the left vector of the camera and the overlap distance, the next viewpoint is projected. This approach is repeated throughout the whole inspection procedure, while the established framework has also the merit to ensure that the inspection path adapts to the shape of the object, which is highly advantageous for the cases of geometrically fractured objects. Multiple realistic and physics based simulation results are presented that prove the efficacy of the proposed scheme.**

***Index Terms*—Keywords: Visual inspection; first-look; Constrained environment; geometrically fractured objects; Kd-tree search.**

I. Introduction

The recent growth in embracing the applications of aerial robotics by the mining and construction industries has generated a tremendous interest in the domain of autonomous operations of UAVs for performing complex tasks, such as visual inspection, mapping and exploration of dangerous and demanding infrastructures. Furthermore, recent studies have been presented towards the inspection of large-scale civil structures, such as bridges and dams [1], [2], wind-turbines and aircrafts [3], [4] that have seen real-life applications of aerial robotics, with an impact towards reducing the danger to human life and increasing productivity and overall performance of the missions.

Currently, the actively addressed topics in constrained environment is on UAV-based exploration and navigation and always in relation with key application sectors. As a very characteristic example, the mining industry is undergoing a paradigm shift in incorporating autonomous vehicles typically having a complex surface geometry, hereby referred to as Geometrically Fractured Objects (GFOs), for safety and rescue operations, extracting and refining resources and removal of excess material from sites to name a few. In such a setup, aerial robots can be used to perform inspection of such heavy machines, which will play a crucial role in maintaining a fleet of such vehicles in the operating conditions, as it is indicated in the concept Figure 1 where a UAV is performing visual inspection of a wheel loader.

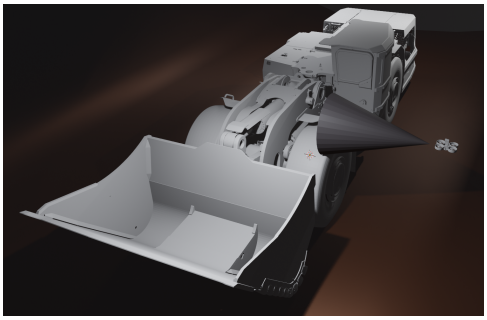

Fig. 1: Concept figure of a GFO oriented aerial visual inspection in a constrained underground environment

In review of the related work, [5] employs a novel $voxel$-based path primitive sampling of offline generated way-points around the target structure, which in this case has been around buildings. The proposed framework produces a shortest inspection path around the target structures that is coupled with modelled coverage constraints, such as a travelling cost between the way-points and the visibility information. In [6], a Coverage Path Planning (CPP) is presented for a sloped dam, which is based on a multi-objective meta-heuristic optimization to meet the photometric constraints within a finite mission duration that also employs a dynamic identification and coverage of prominent features to attain an information rich 3D reconstruction by having the UAV capturing high resolution images of important landmarks. In [7], a volumetric pixel approach supported by GPU-dependent frustum and occlusion culling operations is presented that ensures coverage of external surfaces of an aircraft model using multiple sensors. A Co-optimal Coverage Path Planner (CCPP) presented in [8] is able to holistically optimize both quality of coverage and cost of coverage, while being subject to vehicle constraints of the UAV. In their work, Shang et.al proposes to incorporate a

This work has been partially funded by the illuMINEation Horizon 2020 project from the European Union's Horizon 2020 research and innovation programme under grant agreement No. 869379.

The Authors are with the Robotics and AI Team, Department of Computer, Electrical and Space Engineering, Luleå University of Technology, Luleå

Corresponding Author's email: vigkot@ltu.se

Particle Swarm Optimization (PSO) framework to generate optimal coverage path while satisfying the mission requirements without the need to prioritize inspection objectives.

Based on the previous literature, this article aims to establish it's main contributions towards the domain of visual inspection using aerial vehicles in constrained environments. Firstly, the method of generating view points offline for a visual coverage of a GFO is based on a novel combination of search-space sampling with photogrammetric constraints to ensure coverage quality. The article implements a novel method of model-adaptive view vector orientation, referred to as $First-Look$ approach to generate the next view point based on the current kd-tree Nearest Neighbour. Considering an a priori knowledge of the model, the UAV is controlled to first orient it's viewing axis towards the Nearest Neighbour and then to project the next view point based on the left-vector of the camera on-board and the overlapping distance required. By utilizing a 3D occupancy grid map, the aerial robot is subjected to state-bounds around the point cloud model, restricting it's free space. In order to prevent the generation of view points too close to the surface of the machine or inside the machine, a collision mesh is considered for both the object and UAV, that is validated at each view points. Finally, to validate the proposed framework, realistic physics based GAZEBO simulation has been carried out to validate the proposed method of visual inspection.

The rest of the article is structured as it follows. In Section II the proposed First-Look framework is being presented regarding the extraction of the utilized occupancy grid, the photogrammetric constraints, the nearest neighbour search and the overall control architecture, while in Section III related simulation results that prove the efficacy of the overall presented scheme are depicted. Finally in Section IV the conclusions are drawn.

II. Proposed Framework

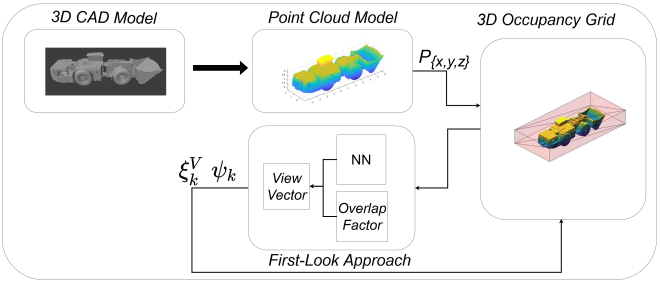

Fig. 2: First-Look enabled Visual Inspection Framework

A. Occupancy Grid

The overall proposed First-Look framework is presented in Fig. 2 where initially the 3D CAD model of the Geometrically Fractured Object is transformed to a dense point cloud model described by $P_{(x,y,z)} \in \mathbb{R}^3$. To construct the operational environment, the 3D occupancy grid map is used to demarcate the available space, where the input point cloud is used to construct a voxel map. As the UAV would perform visual inspection in close quarters to the GFO, a safe operational strategy is detrimental to successfully complete the task. Therefore, a bounding box method is adopted to envelope the object of interest and the UAV in order to avoid collisions. Let $\xi \in \mathbb{R}^3$ be the three-dimensional position of the UAV, given as ξ = [x y z]. The implemented state bounds $B_{3\times2}$ are inherent of the dimensions of the object obtained from $P_{(x,y,z)}$ and of an user-defined matrix of bound distance, $D_{3\times2} = [max(P_{x,y,z}); min(P_{x,y,z})]^T$, where $D_{3\times2} \in \mathbf{R}^{3\times2}$. In Algorithm 1, the related pseudo-code has been provided for the description of the state validation introduced in this article.

Algorithm 1 State Validation

```
Require ξ,B
for i = 1:3 do
    if B(i,1) ≤ ξ_{i×1} ≤ B(i,2) then
        proceed
    else
        flag = sign(ξ_{i×1}) * 1
        if flag > 0 then
            ξ_{i×1} = B(i,2)
        else
            ξ_{i×1} = B(i,1)
        end if
    end if
    Return ξ
end for
```

thus effectively reducing the operational environment to a finite configuration space around the object, $\xi \subseteq \mathbf{B}$. While the bounding box restricts the available space, in order to prevent collision with the object and to ensure a safe operation of the UAV, a cuboidal collision mesh of dimensions $1 \times 1 \times 1$(m) has been considered. Whereas for the vehicle, the mesh dimensions inherit their values according to the bounds of the point cloud along each axes.

B. Photogrammetric Constraints

To ensure for an overall good coverage quality, as depicted in Fig. 3, the required overlap distance $O_H \in \mathbb{R}$ from the current position of the UAV ($T_{pos} \in \mathbb{R}^3$) is modelled to ensure an image overlap from each successive view points. Subjected to a horizontal overlap factor $\gamma_h \in \mathbb{R}$, the horizontal field-of-view of the on-board camera ($\alpha \in \mathbb{R}$) and the nearest point from the model point cloud ($T_{poi} \in \mathbb{R}^3$), the mathematical representation of the required overlap distance is given in (1) as:

$$O_H = 2\tan(\frac{\alpha}{2})||T_{poi} - T_{pos}|| - 2\tan(\frac{\alpha}{2})||T_{poi} - T_{pos}||\gamma_h \quad (1)$$

where for an accurate reconstruction, a $\gamma_h = 0.8$ is preferred. Similarly, the concept of the vertical overlap $O_V \in \mathbb{R}$

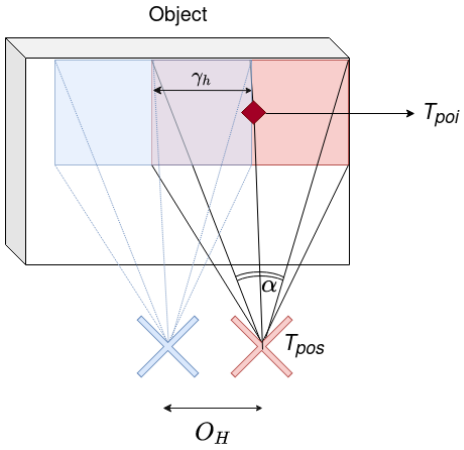

Fig. 3: Front-view showing horizontal overlap between two successive view points

is depicted in Fig. 4. Where $\gamma_v \in \mathbb{R}$ and the vertical field-of-view of $\beta \in \mathbb{R}$ with (2) to indicate the required vertical overlap distance as O_V:

$$O_V = 2\tan(\frac{\beta}{2})||T_{poi} - T_{pos}|| - 2\tan(\frac{\beta}{2})||T\_T_{pos}||\gamma_v \quad (2)$$

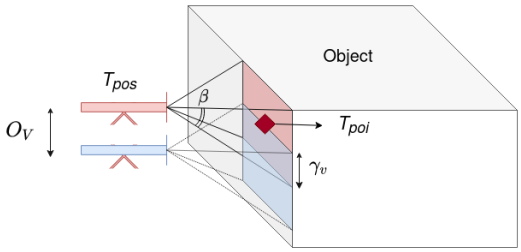

Fig. 4: Side-view showing vertical overlap between two successive view points

C. Nearest Neighbour Search

Common approaches taken towards visual inspection are either an intertwined process of pose optimization, based on a combination of factors, such as information gain, travel cost, dynamic constraints, collision avoidance and a path planner, to obtain the effective and efficient inspection route around the object, while satisfying mission parameters or a way-point generating framework, wrapped in an optimization problem that is subject to similar constraints. Moreover, offline visual inspection by aerial robots is designed to either maintain a constant view direction or having to maintain an orientation to keep looking towards the center of the object [3], without performing either an active vision-based detection of landmark/Point-of-Interest or possessing a-priori knowledge, on the location of such markers, to orient the viewing axis of the UAV. Thus, in Fig. 5, a classical approach to the problem is depicted during the execution of the offline aerial coverage task.

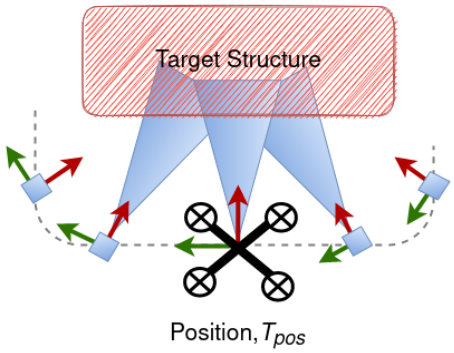

Fig. 5: UAV view orientation realized using Classical approach

To overcome such dependencies in an offline approach, the proposed First-Look method, as depicted in Fig. 6, makes use of the a priori known model information to iteratively address the requirement for an adaptive view orientation that follows the contour of the object under investigation. Furthermore, the article makes use of the Nearest Neighbour (NN) search approach to help providing the desired view vector orientation.

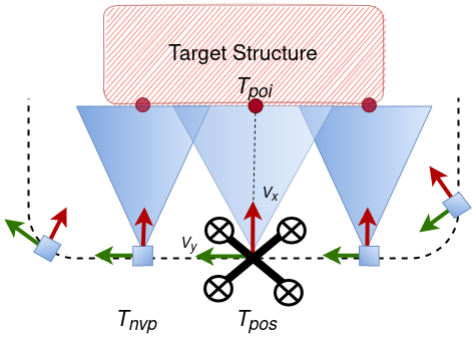

Fig. 6: UAV view orientation realized using proposed $First-Look$ approach

The proposed methodology deviates from standard approaches by deriving the next view point from the current orientation of the UAV, which is a function of the position of the UAV and the point cloud model iteratively, rather than it wholly being an optimization problem or the orientation of the view vector being a function of the position of the UAV solely. Given the point cloud model containing N points, where $p \in P$ and the current position of the UAV (T_{pos}), as the query point, the Euclidean distance between the two points is calculated as:

$$d(p, T_{pos}) = \sqrt{\sum_{i=1}^{N}(T_{pos} - p_i)^2} \quad (3)$$

From (3), it can be seen that as the size of N increases, the computational cost of calculating d also substantially

increases. Therefore, this work utilizes a $kd\ tree$ based Nearest Neighbour search [9]. In general outlook, the provided data points are represented as nodes in a tree and stored in $k\ dimensional$ space. Due to the dense nature of the point cloud being used, the $kd\ tree$ provides a computational advantage over naive neighbour search methodologies, such as the $Brute\ Force$ by not having to compute $d(p, T_{pos})$ $\forall$ $\mathrm{P}_{(x,y,z)}$, but rather employing $O(\log(N))$ calculation of distances. Once **min** $d(p, T_{pos})$ is identified as T_{poi}, the view vectors for the UAV is formulated as:

$$\vec{V_x} = \frac{T_{poi} - T_{pos}}{||T_{poi} - T_{pos}||} \tag{4}$$

$$\vec{V_y} = \vec{U} \times \vec{V_x} \tag{5}$$

$$\vec{V_z} = \vec{V_x} \times \vec{V_y} \tag{6}$$

where, $\vec{U}$ is the vector representing the up direction of the camera given as [0 0 1]. Once the view vectors, $\vec{V_x}$ and $\vec{V_y}$ have been established from the current T_{pos}, the required yaw angle $\theta \in \mathbb{R}$ and the next view point, $\mathrm{T}_{nvp} \in \mathbb{R}^3$ can be formulated as:

$$\theta = \mathrm{atan2}(V_x(2,1), V_x(1,1)) \tag{7}$$

$$T_{nvp} = T_{pos} + V_y O_H \tag{8}$$

To satisfy a vertical overlap and to complete the inspection tour of the object along the vertical axis, the planner derives the operational height of the inspection procedure from the point cloud model provided. Given the known camera parameter α, and $max(P_z)$ of the point cloud model, an initial starting height is calculated considering that the UAV takes-off from the top of the machine via:

$$H_0 = max(P_z) - \arctan(0.5\alpha)(||T_{poi} - T_{pos}||) \tag{9}$$

where, (9) is the initial inspection height that coincides the top of the machine with the top of the view plane projected from the camera. As the inspection proceeds to complete the coverage at the H_0, the next inspection height, H_{insp} is calculated by satisfying mission constraints, such as the safety height denoted as H_{safety} to prevent the UAV from colliding with the ground and the vertical overlap, O_V to meet the overall coverage quality. Thus, (8) can be rewritten as:

$$H_{insp} = H_0 + V_z O_V \tag{10}$$

This method ensures that the UAV is always given view points depending on the orientation of the view vectors, which in turn are dependent on the point cloud model provided. Thus, the offline visual inspection procedure becomes adaptable to the a priori known model at hand, provided the available state space is also modelled accordingly. The provided pseudo-code in the Algorithm 2 describes the overall framework of the proposed $First - Look$ enabled visual inspection.

Algorithm 2 Visual Inspection Planner

```
T_ref = T_pos
while Mission Active do
    Check T_pos for collision
    if Collision Flag true then
        Re-sample within state bounds
    end if
    Find the view direction and calculate O_H, establish next view point, T_nvp
    if ||T_pos − T_ref|| < O_H then
        Proceed to next H_insp
        T_ref = T_pos
        counter = counter + 1
    end if
    if H_insp < H_safety then
        Break
    end if
    T_pos = T_nvp
end while
```

D. Control Architecture

The implemented First-Look framework is a closed loop framework that is based on the control architecture depicted in Fig. 7. Once the required states are generated as previously discussed in Section.II, they are passed onto the Nonlinear Model Predictive Controller (MPC) through the ROS framework. The reference publisher receives the reference states, position and yaw angle from $MATLAB$ and using ROS commands the MPC to provide the required thrust commands to meet the desired pose. Information on the state of the UAV is provided by a simulated Inertial Measurement Unit (IMU) sensor on-board, while more information on the utilized UAV equations and the related MPC scheme can be found in [10].

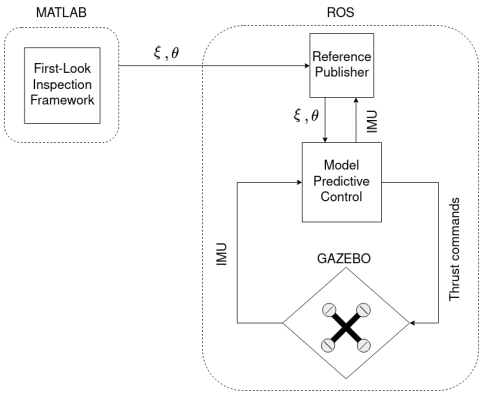

Fig. 7: The overall First-Look closed loop architecture based on MPC

III. Simulation Results

Considering a 3D CAD model of a GFO, the use-case for this article is to implement a visual inspection procedure around it, where the UAV is assumed to take off from the

top of the machine and besides the cabin at an initial position of T_{pos} = [-0.86 -0.7 2.2]. as it is presented in Fig.8. The

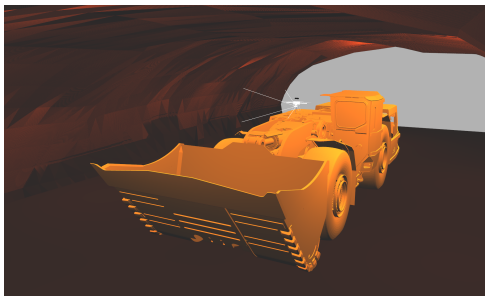

Fig. 8: Simulation environment implemented in GAZEBO

voxel resolution of the 3D occupancy grid was selected to be 15 cells per meter with the model point cloud being dense in nature with 1000080 points. Furthermore, to reduce the image blur, due to the UAV's motion, the UAV is commanded to stabilize itself at each viewpoint for a period of 0.5s, before proceeding onto the next viewpoint. For the simulated scenarios considered, Table I depicts the specifications of the simulated on-board the UAV optical sensor.

α	69.4	degrees
β	42.5	degrees
Image width	640	pixels
Image height	480	pixels
γ_h	0.8	
γ_v	0.6	

TABLE I: Camera specification onboard the UAV

The simulated constrained environment has a length of $20m$ and a width and height of $6m$ and $4m$ respectively, while Table II presents the corresponding bounding conditions of the states.

Axis	Min	Max	Unit
X	min(X)-2	max(X)+2	(m)
Y	min(Y)-2	max(Y)+2	(m)
Z	min(Z)+0.5	max(Z)	(m)

TABLE II: Tabular information on the state bounding box utilized

Fig. 9a provides information on the referenced and closed loop (executed) orientation of the camera view vector and for a single pass around the GFO. As it can be observed from the obtained results, the orientation of the view vector tends to follow the contour of the model provided with minor deviations noticed along the sections, where a cavity or protrusions are present. These anomalies are due to the implemented search environment for the Nearest Neighbour. Currently, the Nearest Neighbour is modelled to search the entire point cloud model $P_{(x,y,z)}$ provided and as such this results in the above observed deviations. Moreover, the executed orientation of the viewing axis can be seen closely following the commanded orientation.

The comparative representation between the reference path obtained from the First-Look presented algorithm and the executed simulated inspection path taken by the UAV around the GFO is presented in Fig. 10. The proposed framework can be seen to generate collision-free paths, while still satisfying the imposed inspection constraints. From Fig. 10, the shape of the inspection path can be seen evolving to the boundary of the modelled state-bounds in II. It should also be noted that due to the shape of the GFO, the adaptive-nature of the method causes the required overlap distance to not be consistent and can be seen varying depending on the position of the UAV from the GFO. This can also be inferred from the offset of the final position compared to the initial position of the UAV. This reinforces the adaptive nature of the visual inspection framework presented in this work.

Furthermore, Fig. 9b depicts the variation in orientation of the viewing axis between the proposed $First-Look$ approach and the classical approach taken during a single pass at an altitude of $-0.69m$. As it can be inferred from the obtained results, the proposed approach generates view orientations that look towards the local region of inspection rather than the constant center-look orientation generated by the classical approach [3]. This allows an information rich dataset to be captured by the UAV, which can then be used to create a 3D mesh of the inspected object.

Finally, Fig. 11 provides a sample pictorial dataset taken by the UAV executing the visual inspection mission around the Geometrically Fractured Object and at the same viewpoints during a single pass as discussed in Fig. 9b previously. From the images, it can conclusively be seen that the proposed framework provides an orientation that covers the local region being inspected, while the classical approach faces the drawback of not being able to adaptively orient it's view vector based on the model point cloud.

IV. Conclusions

In this article a novel offline, model-based aerial visual inspection scheme for geometrically fractured large objects, based on fully autonomous Unmanned Aerial Vehicles (UAVs), while specifically targeting the case of constrained environments has been presented. The proposed framework enabled for a safe and collision free inspection mission, while guaranteeing a complete visual inspection of the object of interest. The proposed framework employed the suggested novel $First-Look$ approach to generate viewpoints while satisfying specific photogrammetric requirements, as well as spatial constraints that are inherently applied by the UAV's state constraints. The presented $First-Look$ approach allows the UAV to: i) orient it's view vector towards the nearest available point detected by $kd-tree$ based Nearest Neighbour search on the object, from it's current position, and ii) in the sequel, based on the orientation of the left vector of the camera and the overlap distance, the next viewpoint is projected. This approach is repeated throughout the whole inspection procedure, while the established framework has also the merit to ensure that the inspection path adapts to the shape of the object, which is highly advantageous for the cases of geometrically fractured objects. The efficiency of the proposed

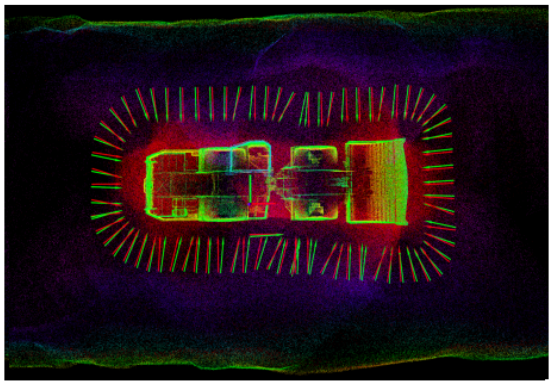

(a) *Rviz* visualization of modelled ($red\ arrow$) and executed pose($green\ arrow$) around the GFO at an altitude of -0.69m

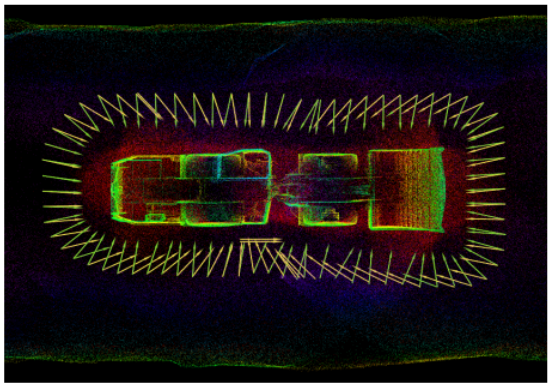

(b) *Rviz* visualization of the comparison presented between the orientation generated using $First - Look$ approach ($green\ arrow$) and Classical approach ($yellow\ arrow$)

Fig. 9: Graphical visualization and comparison of view-orientation maintained during visual inspection of a Geometrically Fractured Object

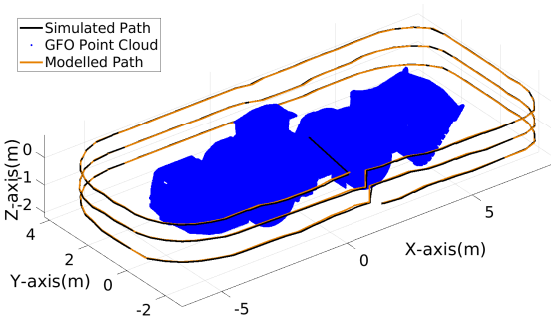

Fig. 10: Graphical representation between the First-Look reference path provided and the executed closed loop path by the UAV

scheme has been successfully evaluated based on extended simulated results.

Fig. 11: For the 40^{th} view point, comparison from the onboard camera view from the $First - Look$ (top) and the classical approach (bottom)

REFERENCES

[1] A. Khaloo, D. Lattanzi, A. Jachimowicz, and C. Devaney, "Utilizing uav and 3d computer vision for visual inspection of a large gravity dam," *Frontiers in Built Environment*, vol. 4, p. 31, 2018.

[2] S. Jung, S. Song, S. Kim, J. Park, J. Her, K. Roh, and H. Myung, "Toward autonomous bridge inspection: A framework and experimental results," in *2019 16th International Conference on Ubiquitous Robots (UR)*. IEEE, 2019, pp. 208–211.

[3] S. S. Mansouri, C. Kanellakis, E. Fresk, D. Kominiak, and G. Nikolakopoulos, "Cooperative coverage path planning for visual inspection," *Control Engineering Practice*, vol. 74, pp. 118–131, 2018.

[4] P. Silberberg and R. C. Leishman, "Aircraft inspection by multirotor uav using coverage path planning," in *2021 International Conference on Unmanned Aircraft Systems (ICUAS)*. IEEE, 2021, pp. 575–581.

[5] W. Jing, D. Deng, Z. Xiao, Y. Liu, and K. Shimada, "Coverage path planning using path primitive sampling and primitive coverage graph for visual inspection," in *2019 IEEE/RSJ International Conference on Intelligent Robots and Systems (IROS)*. IEEE, 2019, pp. 1472–1479.

[6] I. Z. Biundini, M. F. Pinto, A. G. Melo, A. L. M. Marcato, L. M. Honório, and M. J. R. Aguiar, "A framework for coverage path planning optimization based on point cloud for structural inspection," *Sensors*, vol. 21, no. 2, 2021. [Online]. Available: https://www.mdpi.com/1424-8220/21/2/570

[7] R. Almadhoun, T. Taha, J. Dias, L. Seneviratne, and Y. Zweiri, "Coverage path planning for complex structures inspection using unmanned aerial vehicle (uav)," in *International Conference on Intelligent Robotics and Applications*. Springer, 2019, pp. 243–266.

[8] Z. Shang, J. Bradley, and Z. Shen, "A co-optimal coverage path planning method for aerial scanning of complex structures," *Expert Systems with Applications*, vol. 158, p. 113535, 2020.

[9] J. L. Bentley, "Multidimensional binary search trees used for associative searching," *Communications of the ACM*, vol. 18, no. 9, pp. 509–517, 1975.

[10] B. Lindqvist, S. S. Mansouri, and G. Nikolakopoulos, "Non-linear mpc based navigation for micro aerial vehicles in constrained environments," in *2020 European Control Conference (ECC)*. IEEE, 2020, pp. 837–842.